

The spatiotemporal development of adipose tissue

Jinah Han^{1,2,*}, Jung-Eun Lee^{1,2,*}, Jongho Jin¹, Joon Seo Lim¹, Nuri Oh^{1,2}, Kyuho Kim^{1,3}, Soo-Il Chang³, Masabumi Shibuya⁴, Honsoul Kim^{1,3} and Gou Young Koh^{1,2,3,†}

SUMMARY

Adipose tissue is a structure highly specialized in energy storage. The adipocyte is the parenchymal component of adipose tissue and is known to be mesoderm or neuroectoderm in origin; however, adipocyte development remains poorly understood. Here, we investigated the development of adipose tissue by analyzing postnatal epididymal adipose tissue (EAT) in mouse. EAT was found to be generated from non-adipose structure during the first 14 postnatal days. From postnatal day 1 (P1) to P4, EAT is composed of multipotent progenitor cells that lack adipogenic differentiation capacity in vitro, and can be regarded as being in the 'undetermined' state. However, the progenitor cells isolated from P4 EAT obtain their adipogenic differentiation capacity by physical interaction generated by cell-to-matrix and cell-to-cell contact both in vitro and in vivo. In addition, we show that impaired angiogenesis caused by either VEGFA blockade or macrophage depletion in postnatal mice interferes with adipose tissue development. We conclude that appropriate interaction between the cellular and matrix components along with proper angiogenesis are mandatory for the development of adipose tissue.

KEY WORDS: Adipose tissue, Adipogenesis, Angiogenesis, Mouse

INTRODUCTION

Adipose tissue is the only tissue that is able to change its mass substantially even after it reaches the adult size (Spiegelman and Flier, 1996; Hausman et al., 2001). Since the primary role of adipose tissue is energy storage, the adipocyte can indeed change its size dynamically according to the amount of lipid stored, as long as the energy intake exceeds the metabolic demands (Rosen and Spiegelman, 2006). Although increase in adipocyte size is a major component of adipose tissue mass increase, there is a physical limit to how large an adipocyte can become and de novo generation of adipocytes by adipogenesis is required (Rosen and Spiegelman, 2000; Gesta et al., 2007). Even if the number of adipocytes is to remain constant in adulthood, adipogenesis is essential for adipocyte turnover and maintenance of adipose tissue (Spalding et al., 2008). Unfortunately, the structural and functional processes of adipogenesis during development and under obese conditions are poorly understood. In addition, molecular and cellular mechanisms of adipogenesis in vivo are largely unknown because the cellular identities of adipocyte stem cells, adipoblasts, adipocyte progenitors and preadipocytes, as well as their biomarkers (Hauner and Löffler, 1987), have yet to be accurately described.

Adipogenesis is a two-step process: determination of the pluripotent stem cells to the adipocyte lineage to generate so-called preadipocytes, and differentiation of preadipocytes into adipocytes (Rosen and MacDougald, 2006). Numerous studies of adipogenesis have been performed by assessing the preadipocyte cell lines 3T3-L1 and 3T3-F442A after adipogenic induction by reagent treatment

in vitro (Pittenger et al., 1999; Rangwala and Lazar, 2000; Rosen and MacDougald, 2006). The cellular transition of preadipocytes during differentiation comprises four steps: growth arrest, clonal expansion, early differentiation, and terminal differentiation (Gregoire et al., 1998; Rosen and MacDougald, 2006). Extensive studies have been carried out to describe the molecular mechanism and the sequential cascades involved in these procedures (Rangwala and Lazar, 2000; Rosen and Spiegelman, 2000; Rosen et al., 2002; Farmer, 2006), and have identified CCAAT/enhancer binding protein (C/EBP) family and peroxisome proliferator activated receptor γ (PPAR γ) as master regulators for these processes.

Adipocytes generated through adipogenesis compose the adipose tissues in the body. Several reports have revealed the multifarious interaction between angiogenesis and the adipose tissue development process by conducting implantation of preadipocyte cell lines with or without synthetic materials such as Matrigel (Kawaguchi et al., 1998; Rupnick et al., 2002; Neels et al., 2004; Lijnen et al., 2006). We have previously reported that a dense vascular network is formed by angiogenesis in the tip portion of epididymal adipose tissue (EAT) in adult mice, and that the newly formed vascular structure provides the functional route for adipogenesis (Cho et al., 2007). Although valuable insights into adipogenesis and angiogenesis have been provided through these efforts, inevitable limitations remain: first, a preadipocyte cell line is not able to recapitulate the progress of adipogenesis as a whole in a spatiotemporal manner; second, adipogenic induction performed in vitro cannot mimic adipogenesis at the tissue level in vivo (Soukas et al., 2001).

Here, we describe our observations on mouse EAT undergoing postnatal development, and report that adipogenesis takes place in non-adipose structures that are composed of progenitor cells. We also show that angiogenesis has a regulatory role in adipose tissue development.

MATERIALS AND METHODS

Animals

Pathogen-free C57BL/6J (B6) mice (Jackson Laboratory) and GFP⁺ mice (B6 genetic background) (gift from Dr Masaru Okabe, Osaka University, Japan) were used in this study. *Vegfr1* tyrosine kinase knockout (VEGFR1

¹National Research Laboratory of Vascular Biology and Stem Cells, Korea Advanced Institute of Science and Technology (KAIST), Daejeon, 305-701, Korea. ²Department of Biological Sciences, Korea Advanced Institute of Science and Technology (KAIST), Daejeon, 305-701, Korea. ³Graduate School of Medical Science and Engineering, Korea Advanced Institute of Science and Technology (KAIST), Daejeon, 305-701, Korea. ⁴Department of Molecular Oncology, Tokyo Medical and Dental University, Tokyo, 113-8519, Japan.

*These authors contributed equally to this work

†Author for correspondence (gykoh@kaist.ac.kr)

TK KO) mice were generated as previously described (Hiratsuka et al., 1998) and crossbred with the B6 background for more than 20 generations. All mice were bred in our pathogen-free animal facility, and 1- to 14-day postnatal (P1 to P14) and 8-week-old adult male mice were used for this study. Animal care and experimental procedures were performed under approval from the Animal Care Committee of KAIST. All mice were provided with water and a standard diet (PMI LabDiet, Purina Mills), and were anesthetized by an intramuscular injection with a combination of anesthetics (80 mg/kg ketamine and 12 mg/kg xylazine) before sacrifice.

Morphometric and histological analysis

Tissues were fixed using 1% or 4% paraformaldehyde (PFA) diluted in PBS, whole-mounted or cryo-embedded, then sectioned for histological analysis. For further staining, tissues were incubated for 1 hour at room temperature with blocking solution containing 5% donkey serum (Jackson ImmunoResearch) in TBS-T (Tris-buffered saline containing 0.3% Triton X-100). After blocking, the samples were incubated overnight at 4°C with primary antibodies (Table 1). After several washes with TBS-T, the samples were incubated for 4 hours at room temperature with secondary antibodies.

BODIPY (Molecular Probes) was used to detect adipocytes and Hoechst 33342 dye (Molecular Probes) was used to detect the nucleus. Hematoxylin and Eosin (H&E) staining was performed according to a standard procedure. Fluorescent signals were visualized and digital images were obtained using a Zeiss inverted microscope and a Zeiss LSM 510 confocal microscope equipped with argon and helium-neon lasers. Morphometric analyses of adipocytes and blood vessels of EAT were performed using ImageJ software (NIH) or Zeiss image analysis software (AIM and AxioVision). The distributions of adipocytes and blood vessels in EAT were measured in at least three regions per group.

Isolation of stromal vascular fraction (SVF) cells from EAT

SVF cells were harvested as previously reported (Han et al., 2010). Epididymal adipose tissue of B6 and B6 GFP⁺ mice was incubated in Hank's balanced salt solution (HBSS; Sigma-Aldrich) containing 0.2% collagenase type 2 (Worthington) for 45 minutes at 37°C with constant shaking. After inactivating collagenase activity with 10% fetal bovine serum (FBS) in Dulbecco's modified eagle medium (DMEM), the cell suspension was filtered through a 40-μm nylon mesh (BD Biosciences), followed by centrifugation at 420 g for 5 minutes. Floating adipocytes and supernatant were removed from the SVF pellet. The SVF pellet was

washed and resuspended in the medium. Extra precaution was taken during repeated washing with medium considering the nature of adipocytes in developing EAT, which have tiny lipids that are not large enough to be separated by buoyancy, and are thus susceptible to contamination.

mRNA extraction and semi-quantitative RT-PCR

After isolation of total or SVF cells from EAT and harvest of cultured SVF cells at the indicated days, the cells were washed twice with cold PBS. Total RNA was extracted from SVF cells using Trizol (Invitrogen) according to the manufacturer's instructions, and cDNA was synthesized using the SuperScript II First-Strand Synthesis System (Invitrogen). Semi-quantitative PCR was performed with appropriate primers (supplementary material Table S1) using Ex-Taq polymerase (Takara), and the PCR products were visualized on 2% agarose gels containing ethidium bromide.

Phenotypic analysis by flow cytometry

SVF cells were incubated with the antibodies listed in Table 1 [diluted in HBSS containing 2% bovine serum (HBSS buffer)] at 4°C for 15 minutes. After washing, the cells were resuspended in HBSS buffer containing 7-AAD (Molecular Probes). Live lineage-negative cells were analyzed by FACS Aria II (Becton Dickinson) and the data were analyzed using FlowJo (Tree Star).

Adherent or three-dimensional culture and adipogenic induction

For adherent culture, 5×10^4 SVF cells were seeded on a 24-well plate and cultured in DMEM containing 10% FBS (culture medium). One day after cell plating, culture medium was replaced with induction medium [5 μg/ml insulin, 1 μM dexamethasone, 0.5 μM 3-isobutyl-1-methylxanthine (IBMX)] to induce adipogenesis. After 3 days, induction medium was replaced with maintenance medium (5 μg/ml insulin was added to the culture medium) and changed every 3 days until analysis.

For three-dimensional culture, SVF cells were mixed with Matrigel (BD Pharmingen) or growth factor-reduced Matrigel at 3×10^4 cells per 100 μl. Then, 300 μl of cell-gel mixture was plated in a 24-well plate and incubated at 37°C for solidification. When the Matrigel had hardened, induction medium and maintenance medium were added to induce adipogenesis as described above.

For hanging-drop culture, 20 μl drops of hanging-drop medium (culture medium with 0.2% methylcellulose) containing ~3000 SVF cells were hung from the lid of the culture dish. After 3 days, the cell

Table 1. Antibodies

Antibody	Clone	Source
Immunostaining		
Hamster anti-mouse PECAM1	Clone 2H8	Chemicon
Anti-mouse VEGFR2	Polyclonal	Dr Rolf Brekken (University of Texas, Southwestern Medical Center)
Guinea pig anti-mouse perilipin	Polyclonal	Fitzgerald
Rabbit anti-mouse LYVE1	Polyclonal	Upstate
Goat anti-mouse VEGFR3	Polyclonal	R&D Systems
Rabbit anti-human PROX1	Polyclonal	ReliaTech
Rat anti-mouse CD11b	M1/70	BD Pharmingen
Rat anti-mouse F4/80	Cl:A3-1	Serotec
Rat anti-mouse CD68	Polyclonal	Serotec
Flow cytometry		
PE/APC-conjugated anti-mouse CD31	MEC13.3	BD Pharmingen
APC/PerCP-conjugated anti-mouse CD45	30-F11	BD Pharmingen
APC-conjugated anti-mouse TER119 (LY76)	Ter-119	BD Pharmingen
PE-conjugated anti-mouse CD24	M1/69	BD Pharmingen
PE-Cy7-conjugated anti-mouse CD29	HMβ1-1	BD Pharmingen
FITC-conjugated anti-mouse CD34	RAM34	eBiosciences
PE/APC-conjugated anti-mouse SCA1	D7	eBiosciences
PE-conjugated anti-mouse VEGFR2	Avas 12α1	BD Pharmingen
APC-conjugated anti-mouse VE-cadherin	16B1	eBiosciences
Biotin-conjugated anti-mouse c-KIT	2B8	eBiosciences
Streptavidin-APC-Cy7	–	eBiosciences

spheroid was transferred to a 24-well plate and cultured with induction/maintenance medium for 10–14 days. To confirm adipocyte differentiation, Oil-Red O (Chemicon) or BODIPY (Molecular Probes) was used.

Osteogenic and chondrogenic differentiation

To induce osteogenic and chondrogenic differentiation, cultured SVF cells were treated with induction medium as previously described (Zuk et al., 2002; Ogawa et al., 2004). Osteogenic induction medium contained 0.1 μ M dexamethasone, 50 μ g/ml ascorbic acid-2-phosphate and 10 mM β -glycerophosphate; chondrogenic medium contained 10 ng/ml transforming growth factor β 1, 6.25 μ g/ml insulin and 6.25 μ g/ml transferrin. Medium was changed every 3 days. Osteogenic and chondrogenic differentiation were assessed by Alizarin Red (Sigma) and Alcian Blue (Muto Pure Chemicals) staining, respectively.

Colony-forming unit fibroblast (CFU-F) assay

Sorted lineage-negative P4 and adult SVF cells were seeded at 150, 300 and 450 cells per 100-mm plate and cultured to quantify functional mesenchymal stem cells (MSCs). Culture medium was changed every 3–4 days and the number of colonies was assessed 14 days after plating. Cells were fixed for 10 minutes using 1% PFA, washed twice with PBS, and stained with Crystal Violet (Sigma).

VEGF-Trap treatment and macrophage depletion

To inhibit VEGF/VEGFR signaling, postnatal mice were subcutaneously administered with 25 mg/kg VEGF-Trap (Holash et al., 2002; Koh et al., 2010) every other day from P1 to P9, and then sacrificed. For control mice, 25 mg/kg of Fc (a control protein of VEGF-Trap) was injected in the same manner. For systemic depletion of macrophages, mice were treated with intraperitoneal injections of 40 mg/kg clodronate liposome (CDL) (Seiler et al., 1997; Zeisberger et al., 2006) on P3 and P6 and sacrificed on P9. For control mice, empty control liposome (CL) was injected in the same manner.

Statistical analyses

Values are presented as mean \pm s.d. Significant differences between the means were determined by Student's *t*-test or analysis of variance followed by the Student-Newman-Keuls test. Significance was set at $P < 0.05$.

RESULTS

Postnatal development of murine EAT

Various adipose tissues of postnatal mice at different time periods were whole-mounted and stained with BODIPY to examine the distribution of adipocytes. BODIPY staining revealed that the adipocytes of subcutaneous, retroperitoneal and brown adipose

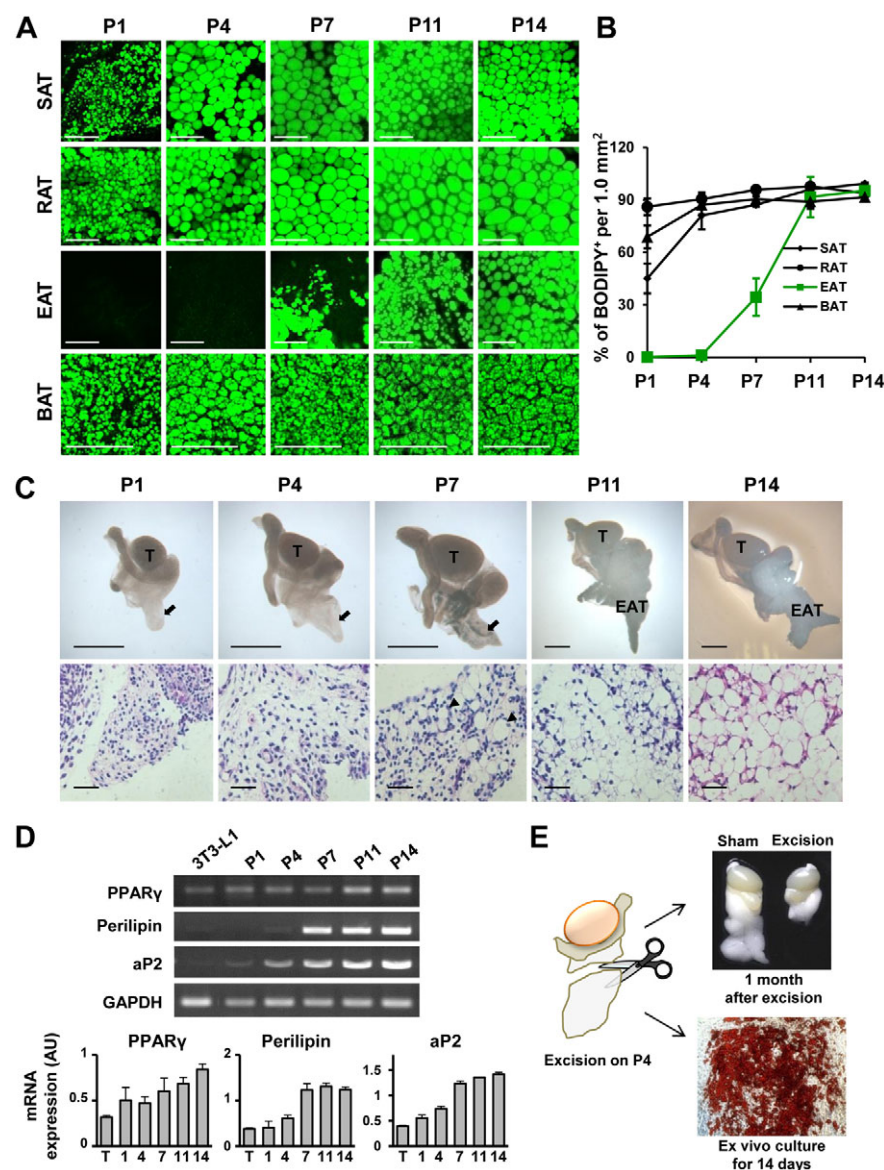


Fig. 1. Postnatal development of murine adipose tissues. (A) BODIPY-stained subcutaneous (SAT), retroperitoneal (RAT), epididymal (EAT) and brown (BAT) adipose tissues from B6 mice. (B) Comparison of BODIPY⁺ adipocyte distribution in each adipose tissue, presented as percentage of BODIPY⁺ adipocytes in total measured area (100 μ m², counted as 100%). Mean \pm s.d.; $n=4$ per group. (C) (Top) Macroscopic images showing EAT at the indicated days. Arrows indicate primitive adipose tissue. T, testis. (Bottom) H&E-stained primitive and matured EAT. Arrowheads indicate matured adipocytes. (D) Representative expression profiles of the adipogenic genes *Pparg*, *perilipin* and *aP2* in EAT. 3T3-L1 cells were cultured by a general adherent culture method. Mean \pm s.d.; $n=3$ per group. The arbitrary unit (AU) value is the expression level of the indicated gene divided by that of the control gene *Gapdh*. (E) Excision of EAT at P4. (Top) Macroscopic image of EAT grown for 1 month after excision or sham operation. (Bottom) Growing Oil-Red⁺ adipocytes from the excised EAT cultured ex vivo for 14 days without adipogenic medium. Scale bars: 100 μ m in A and in C, bottom; 1 mm in C, top.

tissue, already contained lipid components on postnatal day 1 (P1), although the adipocytes themselves were smaller than fully matured adult adipocytes (Fig. 1A,B). By contrast, EAT contained very little, if any, BODIPY⁺ adipocytes until P4; variable sizes of BODIPY⁺ adipocyte started to appear on P7, and fully matured at ~P14 (Fig. 1A,B).

To observe the entire cycle of postnatal adipose tissue development through distinct developmental stages we chose EAT as our platform. Mice between P1 and P14 showed distinct testis and epididymis; the epididymal appendage before P4 seemed premature as it appeared as a thin, translucent membrane-like structure, protruding from beneath the corpus epididymis, later becoming EAT (Fig. 1C, upper panels). H&E sections showed that lipid-filled adipocytes appeared on P7 and gradually replaced the membrane-like structure in a proximodistal manner (Fig. 1C, lower panels).

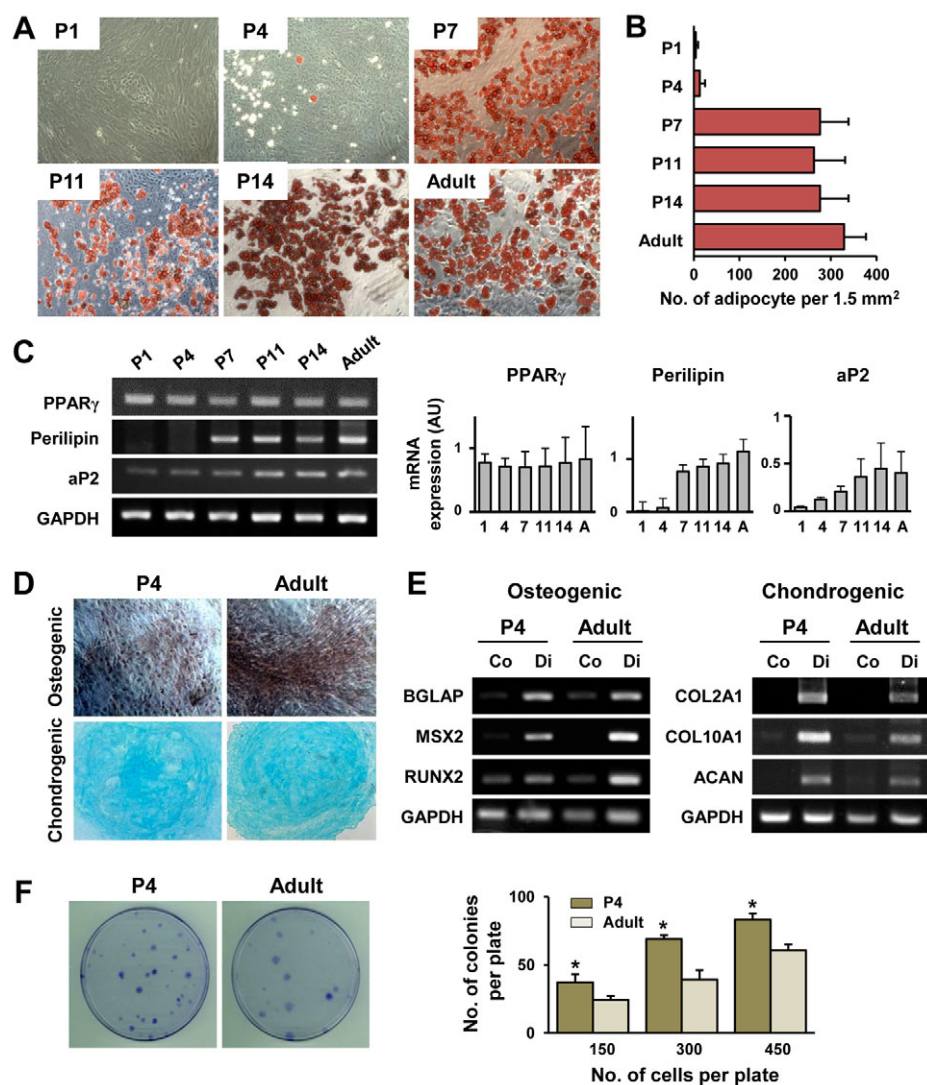
Next, we analyzed the gene expression profiles of adipogenesis by following *Pparg* (which encodes PPAR γ), perilipin and adipocyte protein 2 [*aP2*, also known as fatty acid binding protein 4 (*Fabp4*)] in the postnatal EAT by semi-quantitative (sq) RT-PCR. The expression of these genes gradually increased until P14 (Fig. 1D).

To find out whether the primitive EAT could give rise to adipocytes, we cultured explants of the epididymal appendage before the adipocytes were established and performed in vitro

culture. When cultured with normal medium, the explants of the distal two-thirds of the thin membrane-like structure of the P4 primitive EAT produced numerous lipid-filled adipocytes after 14 days (Fig. 1E). This indicates that the primitive EAT contains adipocyte progenitor cells. Moreover, mice excised of primitive EAT failed to develop mature adipose tissue even after 1 month (Fig. 1E), suggesting that the distal two-thirds of the primitive EAT is necessary for the proper development of adipose tissue.

Progenitor cells derived from primitive EAT have traits of mesenchymal stem cells (MSCs)

To define the chronology of adipogenic potential, SVF cells of mouse EAT at different ages were harvested and cultured with adipogenic induction medium. Notably, cultured SVF cells derived from P1 mice did not give rise to lipid-filled adipocytes, whereas those from P4 mice produced a very low number of lipid-filled adipocytes (Fig. 2A,B). By contrast, cultured SVF cells from P7, P11, P14 and adult mice produced a large number of lipid-containing adipocytes (Fig. 2A,B). The differentiation status of adipocytes derived from the cultured SVF cells was confirmed by analyzing the expression patterns of adipogenic genes, including *aP2*, perilipin and *Pparg*, by sqRT-PCR.



Among these, the expression pattern of perilipin most was closely correlated with the morphologic changes of adipocyte differentiation (Fig. 2A,C).

Based on these findings, we speculated that SVF cells derived from the primitive EAT of mice between P1 and P4 consist of cells that are premature and undetermined compared with those from later developmental stages, and thus named them ‘predetermined progenitor cells’, a term that is roughly equivalent to ‘adipoblasts’ from previous reports (Hauner and Löffler, 1987; Gesta et al., 2007). Naturally, we considered the SVF cells derived from mice older than P7 to be adipocyte progenitor cells. Then, we examined whether the predetermined progenitor cells recapitulated the features of MSCs, as do adipocyte progenitor cells from adult EAT. In fact, the adipocyte progenitor cells from adult adipose tissue are widely accepted as a type of MSC with adipogenic, osteogenic and chondrogenic differentiation capacities (Peng et al., 2008). To assess their osteogenic and chondrogenic differentiation capacities, SVF cells of P4 and adult EAT were cultured with osteogenic and chondrogenic medium for 28 days. Cytochemistry using Alizarin Red and Alcian Blue and sqRT-PCR analysis of expression of osteogenic genes (*Bglap*, *Mx2* and *Runx2*) and chondrogenic genes (*Col2a1*, *Col10a1* and *Acan*) (Vodyanik et al., 2010) revealed that the SVF cells from both P4 and adult EAT had similar levels of osteogenic and chondrogenic differentiation abilities (Fig. 2D,E). Thus, we concluded that the predetermined progenitor cells have the traits of MSCs.

We then performed a colony-forming unit fibroblast (CFU-F) assay on the SVF cells, as fibroblast colony-forming activity is considered to reliably represent the functionality of MSCs as

primitive stem cells in terms of their proliferation capacity (Meirelles Lda and Nardi, 2003). SVF cells derived from both P4 and adult mouse EAT gave rise to fibroblast colonies, but the number of colonies generated from P4 EAT-derived SVF cells was 1.5-fold higher than that of the adult mice. Although we categorized SVF cells from P1 to P4 EAT as MSCs based on their cellular traits, we termed these cells predetermined progenitor cells to distinguish them from the cells of later periods that do show adipogenic potential in vitro. Collectively, these results indicate that SVF cells derived from P4 EAT represent the population of predetermined progenitor cells, which we consider to be potent MSCs that have not yet entered the adipose lineage.

The adipogenic potential of SVF cells derived from postnatal EAT cannot be readily defined by surface markers or the profile of adipose gene expression

To further define the characteristics of SVF cells isolated from EAT as adipocyte progenitor cells, flow cytometry and sqRT-PCR analyses were performed based on descriptions in the literature (Rodeheffer et al., 2008). Flow cytometry data showed that CD34 and CD29 (ITGB1) were expressed at high levels throughout postnatal periods and adulthood, whereas CD24 expression gradually decreased and SCA1 (LY6A) expression increased as the mice aged (Fig. 3A,B). Unexpectedly, the expression profile of these markers on SVF cells did not significantly change between P4 and P7, a period that showed a dramatic change in adipogenic potential in vitro (Fig. 2). Additionally, we assessed whether the

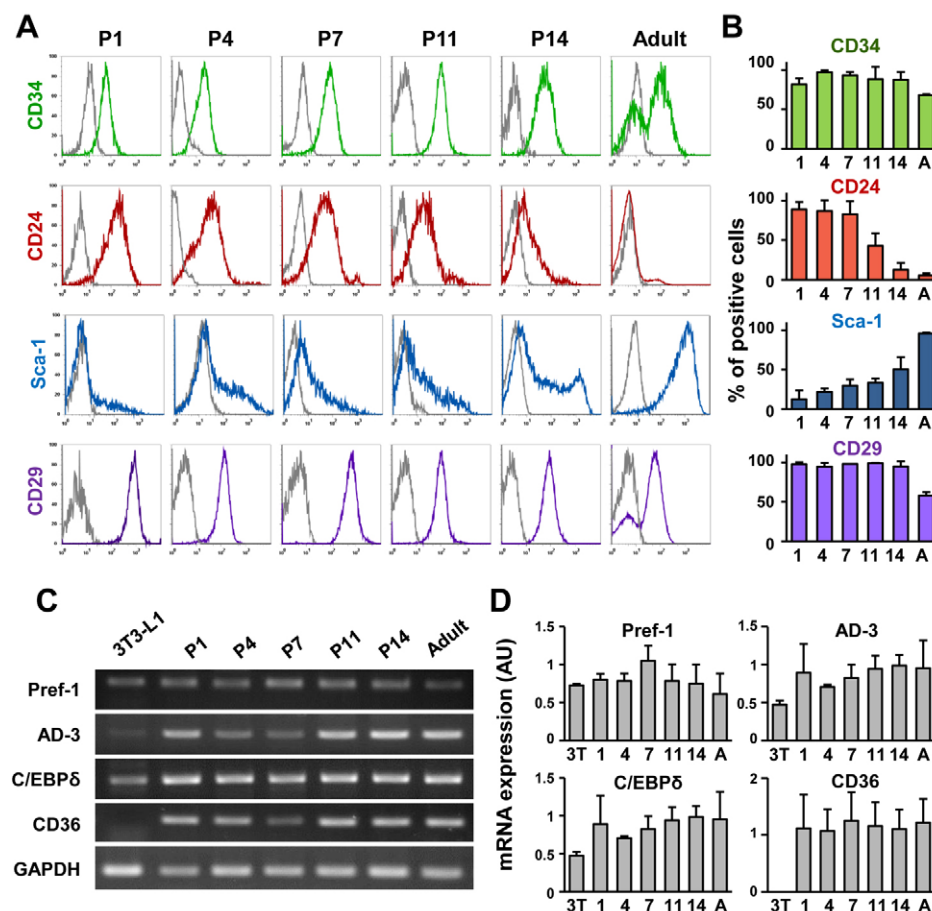


Fig. 3. The adipogenic potential of SVF cells derived from postnatal EAT cannot be described by surface markers or gene expression levels.

SVF cells derived from EAT at the indicated days were analyzed by flow cytometry and semi-quantitative (sq) RT-PCR.

(A) Representative histograms showing expression levels of CD34, CD24, SCA1 and CD29 among the lineage negative population (CD45⁺ Ter119⁺ CD31⁺) of SVF cells. The histogram of the isotype control (gray line) is shown in each case. (B) The percentage of marker-positive cells in the lineage negative population. Mean \pm s.d.; $n=4-7$ per group. (C) Representative sqRT-PCR profiles showing the expression of *Pref1*, *AD-3* and *Cebpd* in adipocyte progenitor cells and *Cd36* in SVF cells. (D) The arbitrary unit (AU) value is the expression level of the indicated gene divided by that of the control gene *Gapdh*. Mean \pm s.d.; $n=3$ per group.

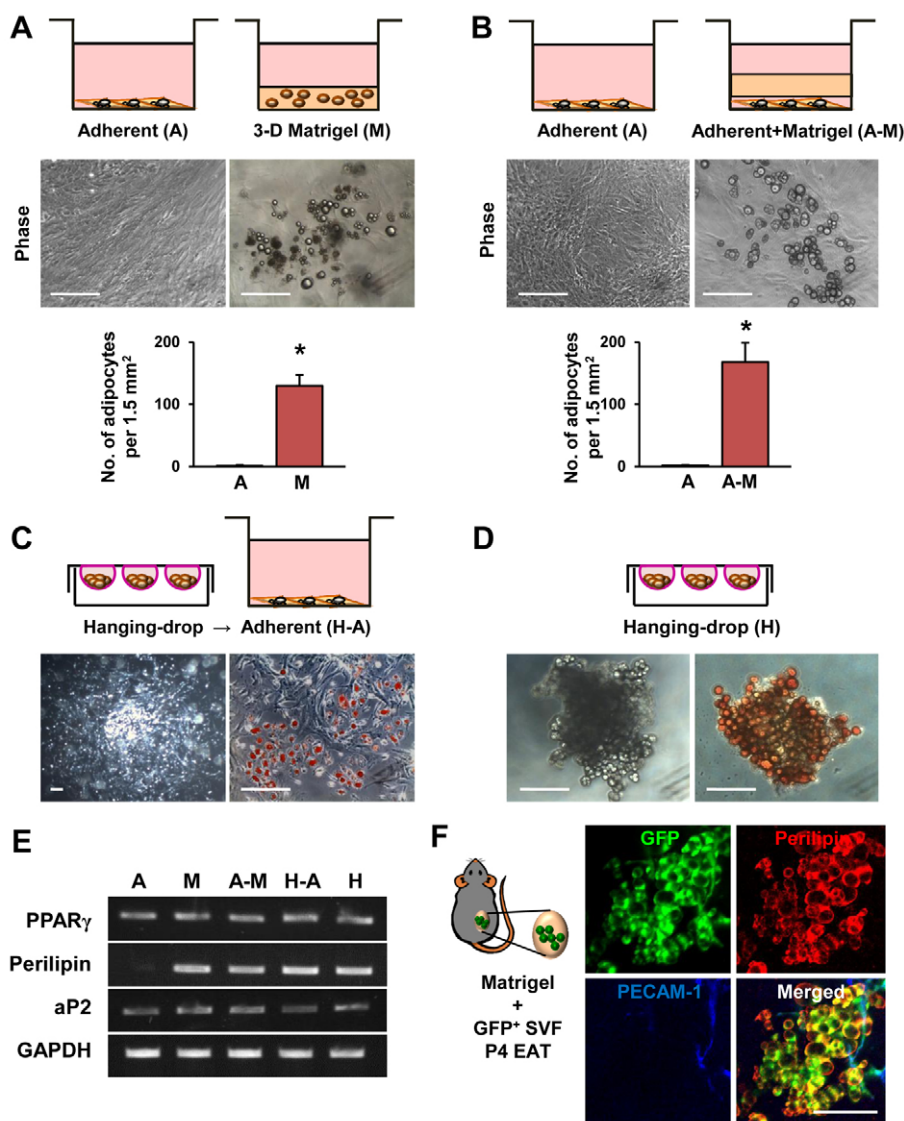
SVF cells expressed markers reported to be expressed on mesoangioblast cells (Cossu and Bianco, 2003; Galvez et al., 2008). Interestingly, the cells expressing mesoangioblast markers [CD31 (PECAM1), CD34, VEGFR2 (KDR), VE-cadherin (cadherin 5), SCA1, c-KIT] were detected in the SVF cells of EAT at different postnatal periods and at adulthood (supplementary material Fig. S1), a finding that needs to be investigated further in the future.

We then performed sqRT-PCR analyses to compare the mRNA levels of genes known to be expressed in adipocyte progenitor cells and during adipogenesis. The expression levels of preadipocyte factor 1 (*Pref1*; *Dlk1*) (Smas and Sul, 1993), *AD-3* (*Tbcl1d8*; a surface antigen that is expressed before adipocyte conversion) (Kras et al., 2000), *Cd36* (a surface glycoprotein that functions as a fatty acid transporter) (Ibrahimi et al., 1996) and *Cebpd* (a transcription factor involved in adipocyte differentiation) (Rosen and Spiegelman, 2000) in EAT-derived SVF cells did not show dynamic changes throughout postnatal development (Fig. 3C,D). These results indicate that the adipogenic potential of the SVF cells derived from postnatal EAT cannot be categorized by the adipogenesis-related surface markers and genes examined in this study.

The primitive SVF cells derived from P4 EAT require cell-to-matrix and cell-to-cell interaction to induce adipogenic determination

We next attempted to elucidate how the predetermined progenitor cells of the primitive EAT from P1 to P4 gain adipogenic potential and transform into adipocyte progenitor cells. Immunohistochemistry of P4 primitive EAT revealed that most of its cells are surrounded by fibronectin-rich extracellular matrix (ECM) (supplementary material Fig. S2A). Previously, protease was reported to play an essential role during three-dimensional adipose tissue development by modulating the adipocyte-ECM interaction (Chun et al., 2006). Based on this report, we hypothesized that the interaction between cells and the surrounding ECM might be crucial for the primitive EAT cells to obtain adipogenic potential. To test this hypothesis, we cultured SVF cells derived from P4 primitive EAT on a fibronectin-coated plate, but adipogenesis was not induced (supplementary material Fig. S2B).

We then addressed whether three-dimensional interaction might be necessary for EAT development, considering its actual conformational structure in vivo, so we simulated a three-dimensional culture environment by embedding the SVF cells



derived from P4 primitive EAT in Matrigel and added adipogenic induction medium on top of the Matrigel (Fig. 4A). These cultures produced numerous variably sized clusters of lipid-containing round adipocytes. Interestingly, lipid-containing adipocytes were more efficiently produced when growth factor-reduced Matrigel was used (supplementary material Fig. S3), a result consistent with a previous report that showed that various growth factors [bFGF (FGF2), EGF, PDGF, TGF β , NGF] contained in Matrigel have an anti-adipogenic effect (Rosen and Spiegelman, 2000).

Based on these observations, we postulated that the physical contact between the predetermined progenitor cells and the surrounding matrix is necessary for adipogenic potential induction. Accordingly, we adopted two different culture systems to determine whether three-dimensional ECM architecture and a certain level of cellular tension is required to maximize adipogenic potential (Fig. 4B-D). Notably, lipid-containing adipocytes were abundantly produced by the addition of Matrigel on top of the attached SVF cells derived from P4 primitive EAT (Fig. 4B) or by hanging-drop culture of SVF cells for 3 days and subsequent adherent culture in the adipogenic medium on a cell plate for 7 days (Fig. 4C). We also noticed that most cells became lipid-containing adipocytes by hanging-drop culture of SVF cells even in the absence of adipogenic medium for 14 days (Fig. 4D). We also examined the expression patterns of adipogenic genes in the differentiated cells produced by different culture methods [adherent (A), Matrigel (M and A-M), and hanging-drop culture (A-H and H)] by sqRT-PCR, and confirmed that these cells were indeed differentiated adipocytes (Fig. 4E).

Next, we explored whether the differentiation of SVF cells into adipocytes by Matrigel implantation was reproducible under *in vivo* conditions. GFP⁺ SVF cells derived from P4 primitive EAT mixed with Matrigel were implanted subcutaneously. Fourteen days after the implantation, SVF cells within Matrigel gave rise to lipid-containing perilipin⁺ adipocytes (Fig. 4F). These data suggest that the predetermined progenitor cells derived from early postnatal EAT require cell-to-matrix or cell-to-cell interaction to achieve their adipogenic character.

Angiogenesis regulated by the VEGF/VEGFR2 system is necessary for adipose tissue development

We expanded our scope of investigation from the cellular to the tissue level. Because angiogenesis precedes adipogenesis/lipogenesis in adult adipose tissues (Cho et al., 2007), we focused on the relationship between adipogenesis and angiogenesis in the primitive EAT during early postnatal development. Well-organized, growing blood vessel networks were observed until P4, but lipid-containing adipocytes were still absent in the primitive membrane structure. On P7, lipid-filled adipocytes of variable size began to appear in clusters on the proximal branches of the vascular network, whereas most of the tip portions of the vascular network remained deprived of lipid-containing adipocytes (Fig. 5A, arrow). In comparison, on P11 and P14, the entire vascular network was abundantly covered with lipid-containing adipocytes (Fig. 5A). Owing to the fact that VEGFA and VEGFC are both derived from stroma and that VEGFR2 and VEGFR3 (FLT4) are specific

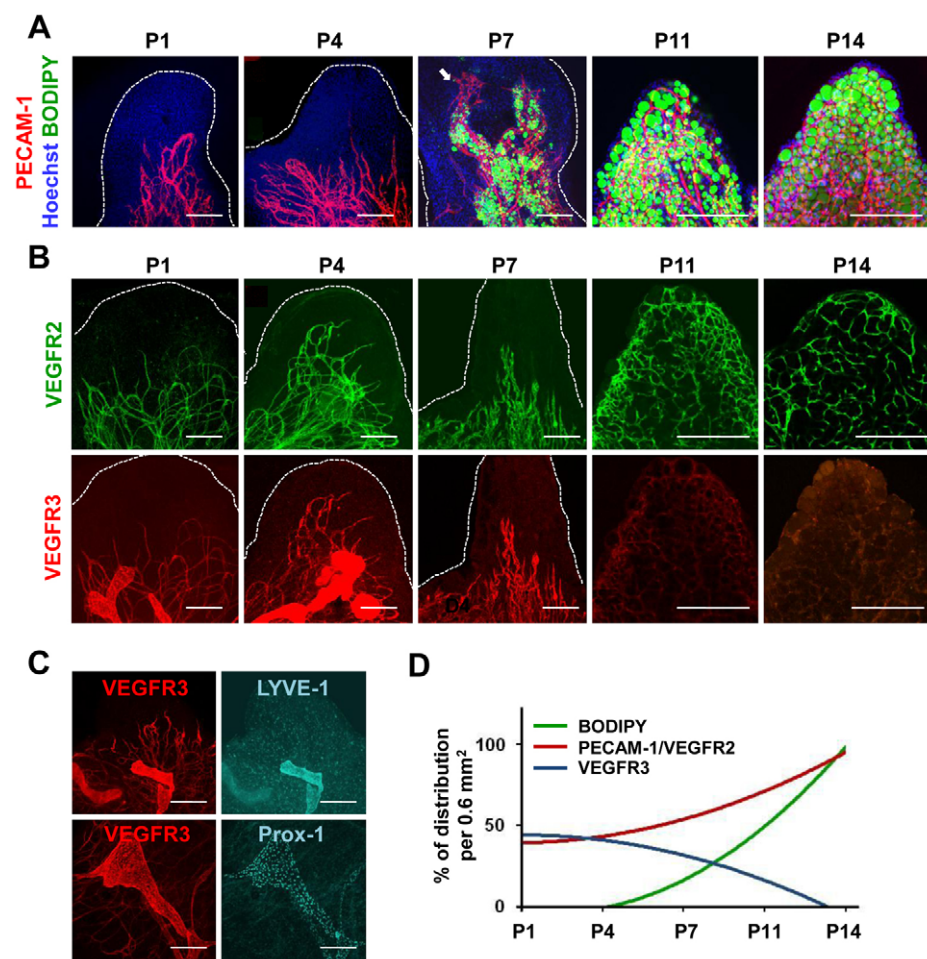


Fig. 5. Angiogenesis precedes adipose tissue development. At the indicated days of postnatal development, adipose tissues of B6 mice were harvested and whole-mount stained to visualize adipocytes, blood vessels, lymphatic vessels and nuclei. (A) The distribution of BODIPY (adipocytes, green), PECAM1 (blood vessels, red) and Hoechst (nucleus, blue) staining in EAT during postnatal development. The white dotted line indicates the margin of the tissue; the arrow indicates angiogenesis preceding adipogenesis. (B) The expression of VEGFR2 (blood vessels, green) and VEGFR3 (blood vessels and lymphatic vessels, red) in EAT. (C) Co-expression of VEGFR3 (red) with LYVE1 and PROX1 (cyan). (D) The average change in BODIPY, PECAM1, VEGFR2 and VEGFR3 in the tip region during postnatal EAT development, presented as a percentage of the total area measured (0.6 mm², counted as 100%). Scale bars: 200 μ m.

receptors for these two respective ligands (Olsson et al., 2006; Adams and Alitalo, 2007), we examined the expression pattern of VEGFR2 and VEGFR3 in the growing vascular networks of EAT. VEGFR2 was highly expressed, mainly in blood vessels, throughout the postnatal period, whereas the expression of VEGFR3 in blood vessels was limited to roughly the first week, followed by marked reduction at P11 and P14 (Fig. 5B,D). VEGFR3 is known to be expressed in all endothelial cells during development, but becomes restricted to lymphatic endothelial cells in adulthood (Tammela et al., 2008). VEGFR3-expressing blood vessels in postnatal EAT reflected the fact that adipose tissue development is accompanied by active angiogenesis. Notably, on P1 and P4, a high level of VEGFR3 was detected in the lymphatic vessels, as verified by LYVE1 (a lymphatic endothelial cell-specific marker) and PROX1 (a transcription factor specific to lymphatic endothelial cells) double immunostaining (Fig. 5C). These data suggest that the VEGFA/VEGFR2 system is closely involved in angiogenesis in EAT development during the early postnatal period.

To identify the role of angiogenesis in EAT development during the early postnatal period, we subcutaneously injected VEGF-Trap (25 mg/kg), an inhibitor of VEGFA and placental growth factor (PlGF; PGF), every other day starting from P1, and performed whole-mount staining to delineate the changes in vascular structure and adipocyte distribution in EAT. On P9, EAT treated with VEGF-Trap displayed a markedly regressed vascular network, with the distal region of EAT remaining avascular, whereas the control EAT became fully vascularized (Fig. 6A,B). Notably, even though BODIPY⁺ adipocytes were detected throughout the entire structure of both control and VEGF-Trap-treated EAT, the sizes of the adipocytes were distinctive: as seen in a magnified view of the distal portion of EAT, adipocytes in EAT treated with VEGF-Trap were considerably smaller, implying delayed adipose tissue development (Fig. 6D,E). In addition, EAT treated with VEGF-Trap showed an

incomplete coverage of adipocytes at the tips of the vascular network, indicating that a premature halt to adipogenesis took place (Fig. 6C). Because the postnatal development of EAT in *Vegfr1* (*Flt1*; which encodes a tyrosine kinase receptor for PlGF) knockout (VEGFR1 TK KO) mice (Hiratsuka et al., 1998; Bais et al., 2010) did not show any difference in vasculature or adipocytes compared with wild-type littermates (supplementary material Fig. S4), we speculate that the adipose tissue remodeling after VEGF-Trap treatment was mainly due to blockade of the VEGFA/VEGFR2 signaling pathway, and not the PlGF/VEGFR1 signaling pathway.

These results, taken together with the spatiotemporal observations of normal EAT development (Fig. 5A), suggest that proper adipogenesis cannot be accomplished unless the preceding angiogenesis is accomplished.

Angiogenic macrophages are an indispensable component of adipose tissue development

LYVE1⁺ macrophages are known to have an angiogenic role in adult EAT via the activation of VEGF, VEGFR2, MMP factors and SDF1 (CXCL12) in an autocrine and paracrine manner (Cho et al., 2007). Since abundant LYVE1⁺ cells were observed in the primitive structure of postnatal EAT (Fig. 7A), we attempted to determine whether LYVE1⁺ cells have a role in angiogenesis and adipogenesis in primitive EAT. Flow cytometry and confocal images clearly demonstrated co-expression of LYVE1 with the macrophage markers F4/80 (EMR1), CD11b (ITGAM) and CD68 on a subpopulation of SVF cells derived from P4 primitive EAT (Fig. 7B,C). We then investigated whether these cells were involved in angiogenesis and adipogenesis during the postnatal period, as is the case in adult EAT. Additional flow cytometric analysis revealed that LYVE1⁺ cells among SVF cells derived from P4 primitive EAT expressed VEGFR1 (41.3±27.0%) and TIE2 (TEK) (77.4±11.1%), which are well-known markers for angiogenic macrophages (Qian and Pollard, 2010). These findings

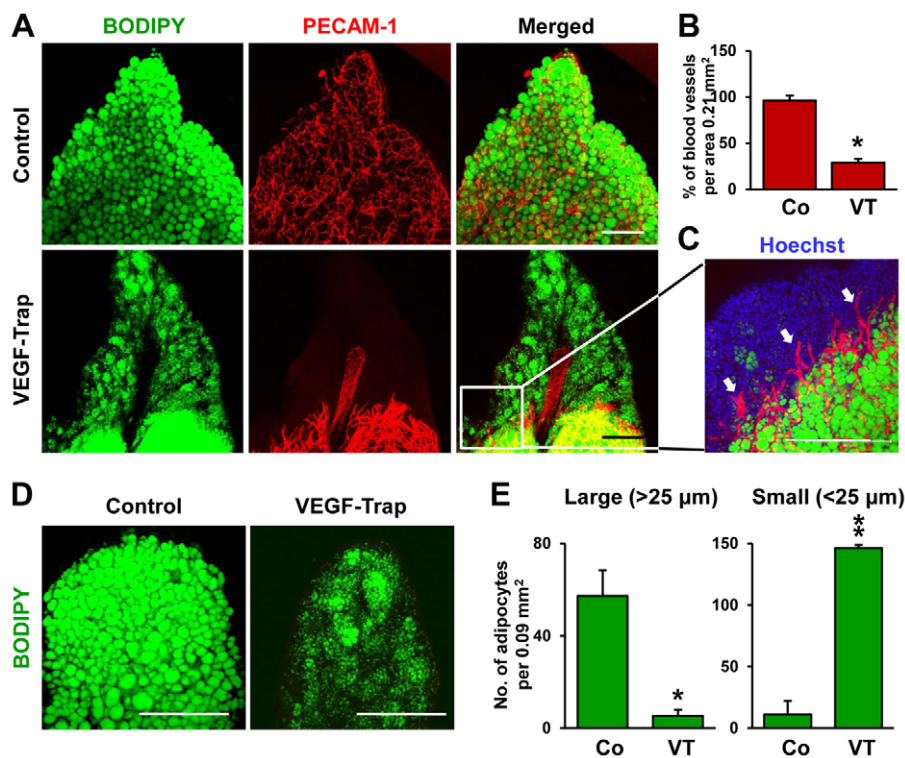


Fig. 6. Angiogenesis regulated by the VEGF/VEGFR2 system is essential for adipose tissue development. Postnatal mice were administered with Fc (25 mg/kg, Control or Co) or VEGF-Trap (25 mg/kg, VT) by subcutaneous injection every other day starting from P1, and sacrificed on P9. (A) Whole-mount stained EAT harvested from control and VEGF-Trap-treated mice. EATs were stained with BODIPY (adipocytes, green), for PECAM1 (blood vessels, red) and with Hoechst (nucleus, blue) and visualized under the confocal microscope. (B) Comparison of blood vessel distribution in the tip region of EAT treated with control and VEGF-Trap, presented as a percentage of the total area measured (0.21 mm², counted as 100%). Mean ± s.d.; n=3 per group; *, *P*<0.05 versus Co. (C) High-magnification view of boxed region in A. Arrows indicate angiogenesis preceding adipogenesis. (D) Comparison of adipocyte size in the tip region of EAT, visualized by BODIPY staining. (E) Large (>25 µm) and small (<25 µm) adipocytes were counted in each 0.09 mm² area of the tip portion of EAT. Mean ± s.d.; n=3 per group. *, *P*<0.05; **, *P*<0.005 versus Co. Scale bars: 200 µm.

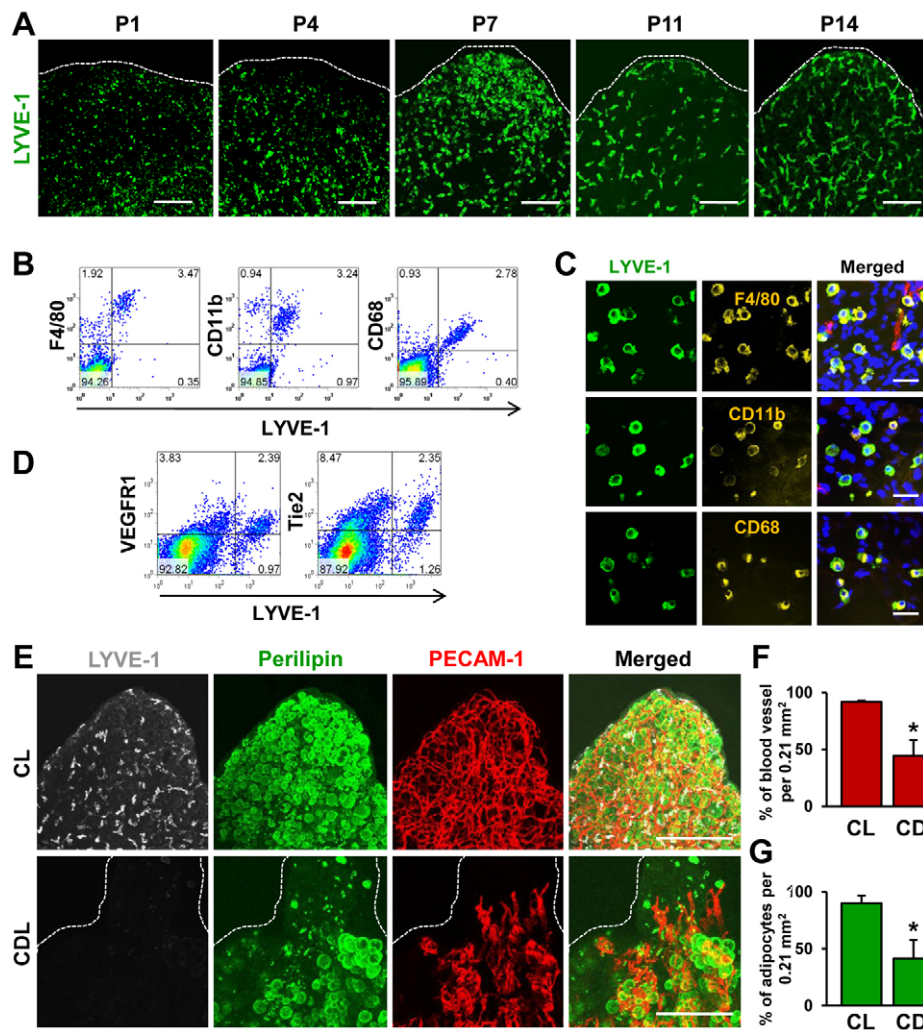


Fig. 7. Angiogenesis regulated by macrophages is supportive of adipose tissue development. At the indicated days of postnatal development, EAT of B6 mice were harvested and analyzed phenotypically and functionally by immunostaining, flow cytometry and by treatment with CL and CDL. **(A)** The distribution of LYVE1⁺ cells (green) in postnatal EAT. **(B,C)** Representative flow cytometric profiles (B) and expression patterns (C) of LYVE1⁺ cells with macrophage markers F4/80, CD11b and CD68. **(D)** Representative flow cytometric profiles showing expression of the angiogenic markers VEGFR1 and Tie2 on LYVE1⁺ cells. **(E)** Mice were administered 40 mg/kg CL or CDL by intraperitoneal injection on P3 and P6, and sacrificed on P9. Whole-mount stained EAT, harvested from CL-treated or CDL-treated mice, showing LYVE1 (macrophage, gray), perilipin (adipocyte, green) and PECAM1 (blood vessels, red). White dotted line depicts the margin of tissue (A,E). **(F,G)** The distribution of blood vessels (F) and adipocytes (G) in the tip portion of CL-treated and CDL-treated EAT, presented as a percentage of the total area measured (0.21 mm², counted as 100%). Mean \pm s.d.; $n=3$ per group; *, $P<0.05$ versus CL. Scale bars: 200 μ m in E; 100 μ m in A; 50 μ m in C.

indicate that LYVE1⁺ cells might be angiogenic macrophages, although the exact function of the surface markers and their mechanisms of action have not been fully identified (supplementary material Fig. S3).

Next, we removed the LYVE1⁺ macrophages to examine the functional role of these cells in angiogenesis in EAT during the postnatal period. Mice were administered with 40 mg/kg CL or CDL (see Materials and methods) by intraperitoneal injection on P3 and P6, and were sacrificed on P9. In the case of CDL-treated EAT, most of the LYVE1⁺ macrophages were successfully eliminated, and very few, if any, LYVE1⁺ macrophages were detectable by whole-mount immunostaining, whereas CL-treated EAT contained abundant LYVE1⁺ macrophages (Fig. 7E). In fact, elimination of macrophages by CDL altered the expression level of several genes, including those encoding bFGF, MMP9, TNF α and TGF β , in whole SVF cells of EAT as compared with those treated with CL (supplementary material Fig. S5). As expected, CDL-treated EAT displayed a marked decrease in the degree and extent of angiogenesis compared with CL-treated EAT (Fig. 7E,F). The distal region, in particular, remained avascular and the coverage of adipocytes was incomplete in CDL-treated mice, whereas extensive vasculature development and adipocyte coverage were achieved in CL-treated mice. We conclude that LYVE1⁺ macrophages have an essential role in angiogenesis and adipogenesis during the postnatal development of EAT.

DISCUSSION

Despite the extensive research carried out on adipogenesis during recent decades, our knowledge in this field remains limited. Here, we used postnatal EAT to demonstrate that adipose tissue development starts from predetermined progenitor cells that initially do not contain lipid, but later give rise to mature adipocytes. Our observations are the first to describe the origin of adipose tissue in vivo and to characterize its development. We categorized the SVF cells isolated from primitive EAT into predetermined progenitor cells and adipocyte progenitor cells according to their in vitro adipogenic potentials. Phenotypic analysis by flow cytometry and gene expression profiles determined by RT-PCR provided a descriptive explanation for the cellular changes that occur during adipose tissue development. Moreover, the role of angiogenesis in adipogenesis and natural adipose tissue development was clearly demonstrated.

The cellular components that correspond to adipocytes in the EAT of P1-P4 mice do not contain lipid droplets and therefore apparently differ from adult adipocytes. Nevertheless, the postnatal primitive EAT becomes gradually replaced with more typical adipocytes within 14 days after birth. Because most of the tissue components determined to turn into adipose tissue are known to develop during the embryonic stage (Hausman and Richardson, 1983; Ailhaud et al., 1992; Crandall et al., 1997) and later become attached to other organs, it would be extremely challenging, if not

technically impossible, to track down the embryonic origin of these tissue components. Therefore, we focused on EAT because it is largely separated from adjacent tissues, with clear demarcation, thus enabling clean isolation of the adipose tissue. This approach allowed us to observe the spatiotemporal dynamics of the entire process of adipose tissue development. Another advantage of this approach is that the excision of the primitive EAT structure enabled us to ascertain that the developmental source of adipocytes is restricted to the original depot, thus excluding the effect of circulating progenitor cells (Crossno et al., 2006; Koh et al., 2007).

One of the main foci of our study was to explore the identity of the cells that comprise the primitive EAT and to establish when their adipogenic fate is determined. Through an in vitro functional assay measuring multilineage differentiation potential, we characterized the SVF cells derived from primitive EAT as containing a population of predetermined progenitor cells that meet the criteria of MSCs, showing several features similar to those of adult EAT (Zuk et al., 2002; Peng et al., 2008) but lacking adipogenic capacity in adherent culture. We found that the fate of these cells remained undetermined between P1 and P4, but they became spontaneously determined as adipocyte progenitor cells after P7.

In spite of such dynamic changes in the adipogenic potential of SVF cells isolated before P4 and after P7, some differences in surface markers and gene expression were observed. Such ambiguity in the classification of SVF cells derived from postnatal EAT remains a limitation in describing the identity of predetermined progenitor cells and adipocyte progenitor cells. We hope that subsequent studies will provide more reliable and technically practical criteria to specify each cell type genetically and/or phenotypically.

We also attempted to identify the conditions required for proper adipogenesis, and demonstrated that adipogenesis cannot be accomplished unless cell-to-matrix and cell-to-cell interaction occur. This observation is relevant to the current concept that the fate of MSCs is influenced by various physical interactions (McBeath et al., 2004; Engler et al., 2006; Guilak et al., 2009). In vitro culture under various conditions demonstrated that predetermined progenitor cells that were attached to a culture dish (and were presumably being stretched) failed to differentiate into adipocytes, whereas cells that were cultured in Matrigel or in the form of clusters (and were presumably protected from being significantly stretched) successfully underwent adipogenesis. Therefore, we believe that the primitive structure of EAT is important not only as the source of progenitor cells, but also as a scaffold that ensures the physical interaction required for the determination of predetermined progenitor cells as adipocyte progenitor cells.

We then identified the guidance role of angiogenesis in adipose tissue development through microscopic approaches. During postnatal EAT development, the growth of blood vessels precedes adipocyte differentiation and maturation (Rajashankar et al., 2008), and, in our study, the contact of adipocyte progenitor cells with blood vessels appeared to be essential during the in vivo adipogenesis of EAT. This led us to conclude that proper angiogenesis is crucial to allow successful adipogenesis in vivo. Moreover, the inhibition of angiogenesis by VEGF-Trap treatment or macrophage depletion caused a definite impairment in the tissue architecture of EAT, which then resulted in interference in adipose tissue development, a finding consistent with previous reports (Rupnick et al., 2002; Brakenhielm et al., 2004; Lijnen et al., 2006; Cao, 2007; Cao, 2010). VEGF-Trap induced small adipocytes to

appear in the avascular region. This could be additional evidence that progenitor cells require appropriate interaction with the surrounding extracellular environment to initiate adipogenesis. Thus, we believe that angiogenesis has a crucial role in the terminal differentiation and maturation of adipose tissue. Nevertheless, we cannot rule out the possibility of impaired differentiation of VEGFR2-expressing common precursor cells (such as the mesoangioblasts that give rise to both mesenchymal and endothelial cells) (Minasi et al., 2002; Vodyanik et al., 2010) into adipocytes due to blockade of VEGFA, rather than direct inhibition of angiogenesis.

In conclusion, our study expands current knowledge concerning adipogenesis by describing the spatiotemporal events during epididymal adipose tissue development. Although the specific mechanisms should be explored further in subsequent studies, we were able to demonstrate that appropriate interaction between the cellular components and the ECM is essential, and that adipogenesis is a sequential process that follows angiogenesis. We account for these phenomena in terms of fate determination, whereby the predetermined progenitor cells become adipocyte progenitor cells and subsequently differentiate into adipocytes.

Acknowledgements

We thank Sujin Seo and Eun Soon Lee for technical assistance; Dr Rolf Brekken for anti-VEGFR2 antibody; and Dr Reto A. Schwendener for clodronate liposome.

Funding

This research was supported by grants from the National Research Foundation (NRF) of the Ministry of Education, Science and Technology (MEST), Korea [2011-0019268 to G.Y.K.]; and the Stem Cell Research Center of the 21st Century Frontier Research Program [SC-5120 to G.Y.K.].

Competing interests statement

The authors declare no competing financial interests.

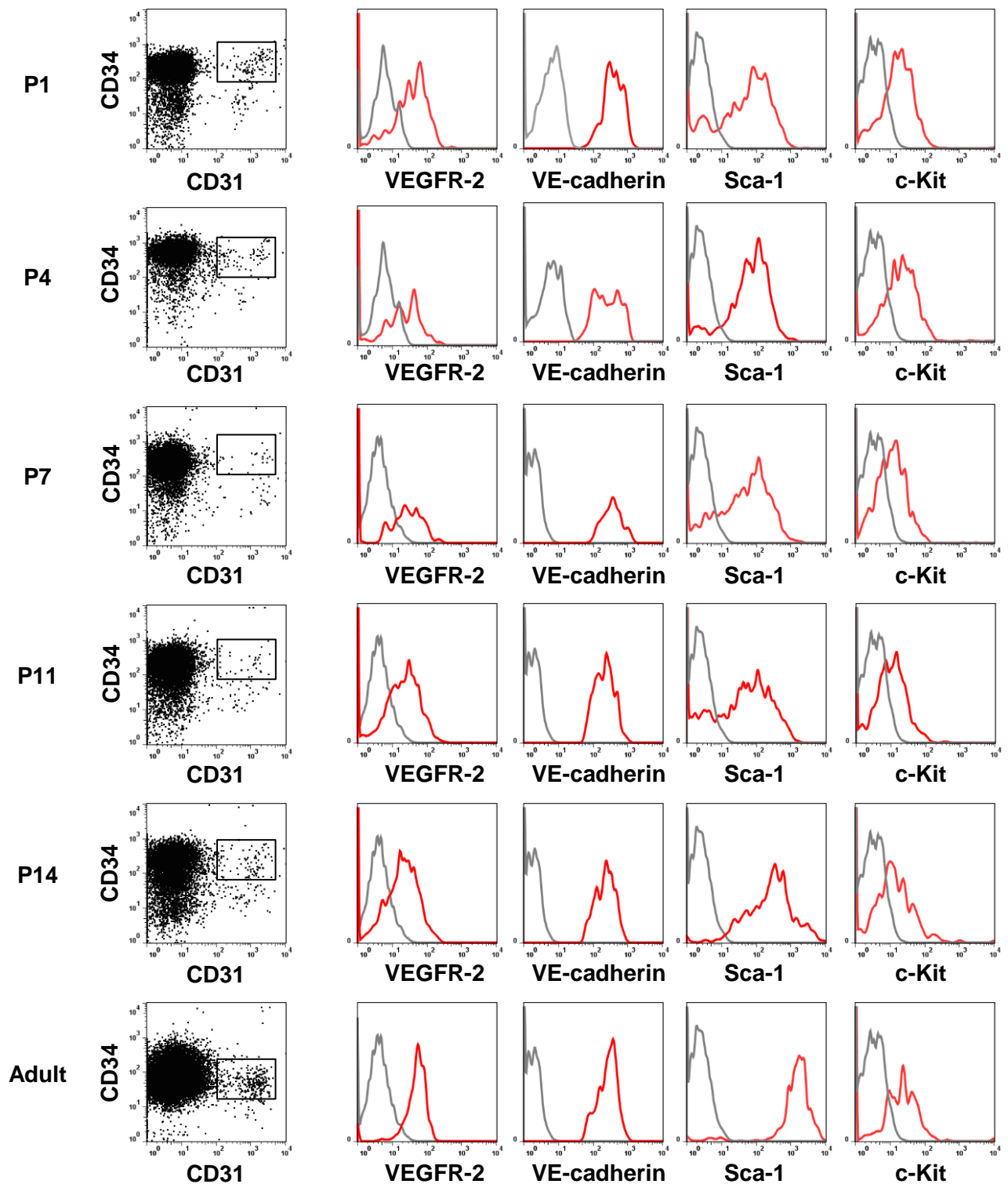
Supplementary material

Supplementary material available online at
<http://dev.biologists.org/lookup/suppl/doi:10.1242/dev.067686/-DC1>

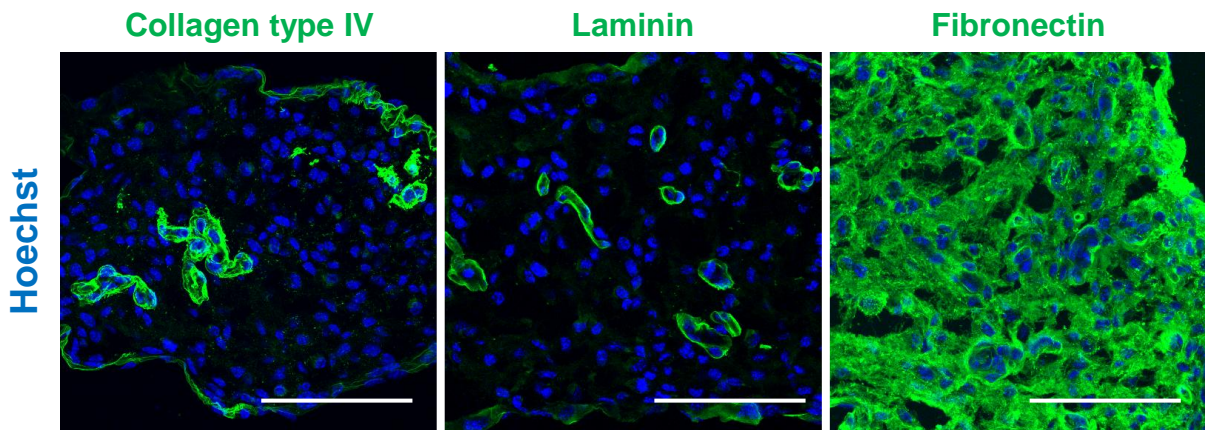
References

- Adams, R. H. and Alitalo, K. (2007). Molecular regulation of angiogenesis and lymphangiogenesis. *Nat. Rev. Mol. Cell Biol.* **8**, 464-478.
- Ailhaud, G., Grimaldi, P. and Negrel, R. (1992). Cellular and molecular aspects of adipose tissue development. *Annu. Rev. Nutr.* **12**, 207-233.
- Bais, C., Wu, X., Yao, J., Yang, S., Crawford, Y., McCutcheon, K., Tan, C., Kolumam, G., Vernes, J. M., Eastham-Anderson, J. et al. (2010). PlGF blockade does not inhibit angiogenesis during primary tumor growth. *Cell* **141**, 166-177.
- Brakenhielm, E., Cao, R., Gao, B., Angelin, B., Cannon, B., Parini, P. and Cao, Y. (2004). Angiogenesis inhibitor, TNP-470, prevents diet-induced and genetic obesity in mice. *Circ. Res.* **94**, 1579-1588.
- Cao, Y. (2007). Angiogenesis modulates adipogenesis and obesity. *J. Clin. Invest.* **117**, 2362-2368.
- Cao, Y. (2010). Adipose tissue angiogenesis as a therapeutic target for obesity and metabolic diseases. *Nat. Rev. Drug Discov.* **9**, 107-115.
- Cho, C. H., Koh, Y. J., Han, J., Sung, H. K., Jong Lee, H., Morisada, T., Schwendener, R. A., Brekken, R. A., Kang, G., Oike, Y. et al. (2007). Angiogenic role of LYVE-1-positive macrophages in adipose tissue. *Circ. Res.* **100**, e47-e57.
- Chun, T. H., Hotary, K. B., Sabeh, F., Saltiel, A. R., Allen, E. D. and Weiss, S. J. (2006). A pericellular collagenase directs the 3-dimensional development of white adipose tissue. *Cell* **125**, 577-591.
- Cossu, G. and Bianco, P. (2003). Mesoangioblasts-vascular progenitors for extravascular mesodermal tissues. *Curr. Opin. Genet. Dev.* **13**, 537-542.
- Crandall, D. L., Hausman, G. J. and Kral, J. G. (1997). A review of the microcirculation of adipose tissue: anatomic, metabolic, and angiogenic perspectives. *Microcirculation* **4**, 211-232.
- Crossno, J. T., Jr, Majka, S. M., Grazia, T., Gill, R. G. and Klemm, D. J. (2006). Rosiglitazone promotes development of a novel adipocyte population from bone marrow-derived circulating progenitor cells. *J. Clin. Invest.* **116**, 3220-3228.
- Engler, A. J., Sen, S., Sweeney, H. L. and Discher, D. E. (2006). Matrix elasticity directs stem cell lineage specification. *Cell* **126**, 677-689.

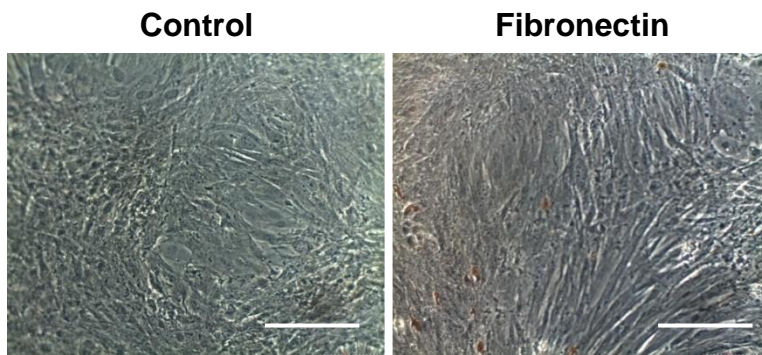
- Farmer, S. R. (2006). Transcriptional control of adipocyte formation. *Cell Metab.* **4**, 263-273.
- Galvez, B. G., Sampaioles, M., Barbuti, A., Crespi, A., Covarello, D., Brunelli, S., Dellavalle, A., Crippa, S., Balconi, G., Cuccovillo, I. et al. (2008). Cardiac mesoangioblasts are committed, self-renewable progenitors, associated with small vessels of juvenile mouse ventricle. *Cell Death Differ.* **15**, 1417-1428.
- Gesta, S., Tseng, Y. H. and Kahn, C. R. (2007). Developmental origin of fat: tracking obesity to its source. *Cell* **131**, 242-256.
- Gregoire, F. M., Smas, C. M. and Sul, H. S. (1998). Understanding adipocyte differentiation. *Physiol. Rev.* **78**, 783-809.
- Guilak, F., Cohen, D. M., Estes, B. T., Gimble, J. M., Liedtke, W. and Chen, C. S. (2009). Control of stem cell fate by physical interactions with the extracellular matrix. *Cell Stem Cell* **5**, 17-26.
- Han, J., Koh, Y. J., Moon, H. R., Ryoo, H. G., Cho, C. H., Kim, I. and Koh, G. Y. (2010). Adipose tissue is an extramedullary reservoir for functional hematopoietic stem and progenitor cells. *Blood* **115**, 957-964.
- Hauner, H. and Loffler, G. (1987). Adipose tissue development: the role of precursor cells and adipogenic factors. Part I: adipose tissue development and the role of precursor cells. *Klin. Wochenschr.* **65**, 803-811.
- Hausman, D. B., DiGirolamo, M., Bartness, T. J., Hausman, G. J. and Martin, R. J. (2001). The biology of white adipocyte proliferation. *Obes. Rev.* **2**, 239-254.
- Hausman, G. J. and Richardson, R. L. (1983). Cellular and vascular development in immature rat adipose tissue. *J. Lipid Res.* **24**, 522-532.
- Hiratsuka, S., Minowa, O., Kuno, J., Noda, T. and Shibuya, M. (1998). Flt-1 lacking the tyrosine kinase domain is sufficient for normal development and angiogenesis in mice. *Proc. Natl. Acad. Sci. USA* **95**, 9349-9354.
- Holash, J., Davis, S., Papadopoulos, N., Croll, S. D., Ho, L., Russell, M., Boland, P., Leidich, R., Hylton, D., Burova, E. et al. (2002). VEGF-Trap: a VEGF blocker with potent antitumor effects. *Proc. Natl. Acad. Sci. USA* **99**, 11393-11398.
- Ibrahim, A., Sfeir, Z., Magharaie, H., Amri, E. Z., Grimaldi, P. and Abumrad, N. A. (1996). Expression of the CD36 homolog (FAT) in fibroblast cells: effects on fatty acid transport. *Proc. Natl. Acad. Sci. USA* **93**, 2646-2651.
- Kawaguchi, N., Toriyama, K., Nicodemou-Lena, E., Inoue, K., Torii, S. and Kitagawa, Y. (1998). De novo adipogenesis in mice at the site of injection of basement membrane and basic fibroblast growth factor. *Proc. Natl. Acad. Sci. USA* **95**, 1062-1066.
- Koh, Y. J., Kang, S., Lee, H. J., Choi, T. S., Lee, H. S., Cho, C. H. and Koh, G. Y. (2007). Bone marrow-derived circulating progenitor cells fail to transdifferentiate into adipocytes in adult adipose tissues in mice. *J. Clin. Invest.* **117**, 3684-3695.
- Koh, Y. J., Kim, H. Z., Hwang, S. I., Lee, J. E., Oh, N., Jung, K., Kim, M., Kim, K. E., Kim, H., Lim, N. K. et al. (2010). Double antiangiogenic protein, DAA, targeting VEGF-A and angiopoietins in tumor angiogenesis, metastasis, and vascular leakage. *Cancer Cell* **18**, 171-184.
- Kras, K. M., Hausman, D. B. and Martin, R. J. (2000). Tumor necrosis factor- α stimulates cell proliferation in adipose tissue-derived stromal-vascular cell culture: promotion of adipose tissue expansion by paracrine growth factors. *Obes. Res.* **8**, 186-193.
- Lijnen, H. R., Christiaens, V., Scroyen, I., Voros, G., Tjwa, M., Carmeliet, P. and Collen, D. (2006). Impaired adipose tissue development in mice with inactivation of placental growth factor function. *Diabetes* **55**, 2698-2704.
- McBeath, R., Pirone, D. M., Nelson, C. M., Bhadriraju, K. and Chen, C. S. (2004). Cell shape, cytoskeletal tension, and RhoA regulate stem cell lineage commitment. *Dev. Cell* **6**, 483-495.
- Meirelles Lda, S. and Nardi, N. B. (2003). Murine marrow-derived mesenchymal stem cell: isolation, in vitro expansion, and characterization. *Br. J. Haematol.* **123**, 702-711.
- Minasi, M. G., Riminucci, M., De Angelis, L., Borello, U., Berarducci, B., Innocenzi, A., Caprioli, A., Sirabella, D., Baiocchi, M., De Maria, R. et al. (2002). The meso-angioblast: a multipotent, self-renewing cell that originates from the dorsal aorta and differentiates into most mesodermal tissues. *Development* **129**, 2773-2783.
- Neels, J. G., Thinnen, T. and Loskutoff, D. J. (2004). Angiogenesis in an in vivo model of adipose tissue development. *FASEB J.* **18**, 983-985.
- Ogawa, R., Mizuno, H., Watanabe, A., Migita, M., Hyakusoku, H. and Shimada, T. (2004). Adipogenic differentiation by adipose-derived stem cells harvested from GFP transgenic mice-including relationship of sex differences. *Biochem. Biophys. Res. Commun.* **319**, 511-517.
- Olsson, A. K., Dimberg, A., Kreuger, J. and Claesson-Welsh, L. (2006). VEGF receptor signalling-in control of vascular function. *Nat. Rev. Mol. Cell Biol.* **7**, 359-371.
- Peng, L., Jia, Z., Yin, X., Zhang, X., Liu, Y., Chen, P., Ma, K. and Zhou, C. (2008). Comparative analysis of mesenchymal stem cells from bone marrow, cartilage, and adipose tissue. *Stem Cells Dev.* **17**, 761-773.
- Pittenger, M. F., Mackay, A. M., Beck, S. C., Jaiswal, R. K., Douglas, R., Mosca, J. D., Moorman, M. A., Simonetti, D. W., Craig, S. and Marshak, D. R. (1999). Multilineage potential of adult human mesenchymal stem cells. *Science* **284**, 143-147.
- Qian, B. Z. and Pollard, J. W. (2010). Macrophage diversity enhances tumor progression and metastasis. *Cell* **141**, 39-51.
- Rajashekhar, G., Traktuev, D. O., Roell, W. C., Johnstone, B. H., Merfeld-Clauss, S., Van Natta, B., Rosen, E. D., March, K. L. and Clauss, M. (2008). IFATS collection: Adipose stromal cell differentiation is reduced by endothelial cell contact and paracrine communication: role of canonical Wnt signaling. *Stem Cells* **26**, 2674-2681.
- Rangwala, S. M. and Lazar, M. A. (2000). Transcriptional control of adipogenesis. *Annu. Rev. Nutr.* **20**, 535-559.
- Rodeheffer, M. S., Birsoy, K. and Friedman, J. M. (2008). Identification of white adipocyte progenitor cells in vivo. *Cell* **235**, 240-249.
- Rosen, E. D. and Spiegelman, B. M. (2000). Molecular regulation of adipogenesis. *Annu. Rev. Cell Dev. Biol.* **16**, 145-171.
- Rosen, E. D. and MacDougald, O. A. (2006). Adipocyte differentiation from the inside out. *Nat. Rev. Mol. Cell Biol.* **7**, 885-896.
- Rosen, E. D. and Spiegelman, B. M. (2006). Adipocytes as regulators of energy balance and glucose homeostasis. *Nature* **444**, 847-853.
- Rosen, E. D., Hsu, C. H., Wang, X., Sakai, S., Freeman, M. W., Gonzalez, F. J. and Spiegelman, B. M. (2002). C/EBP α induces adipogenesis through PPARGamma: a unified pathway. *Genes Dev.* **16**, 22-26.
- Rupnick, M. A., Panigrahy, D., Zhang, C. Y., Dallabrida, S. M., Lowell, B. B., Langer, R. and Folkman, M. J. (2002). Adipose tissue mass can be regulated through the vasculature. *Proc. Natl. Acad. Sci. USA* **99**, 10730-10735.
- Seiler, P., Aichele, P., Odermatt, B., Hengartner, H., Zinkernagel, R. M. and Schwendener, R. A. (1997). Crucial role of marginal zone macrophages and marginal zone metallophilic cells in the clearance of lymphocytic choriomeningitis virus infection. *Eur. J. Immunol.* **27**, 2626-2633.
- Smas, C. M. and Sul, H. S. (1993). Pref-1, a protein containing EGF-like repeats, inhibits adipocyte differentiation. *Cell* **73**, 725-734.
- Soukas, A., Socci, N. D., Saatkamp, B. D., Novelli, S. and Friedman, J. M. (2001). Distinct transcriptional profiles of adipogenesis in vivo and in vitro. *J. Biol. Chem.* **276**, 34167-34174.
- Spalding, K. L., Arner, E., Westermark, P. O., Bernard, S., Buchholz, B. A., Bergmann, O., Blomqvist, L., Hoffstedt, J., Naslund, E., Britton, T. et al. (2008). Dynamics of fat cell turnover in humans. *Nature* **453**, 783-787.
- Spiegelman, B. M. and Flier, J. S. (1996). Adipogenesis and obesity: rounding out the big picture. *Cell* **87**, 377-389.
- Tammela, T., Zarkada, G., Wallgard, E., Murtomaki, A., Suchting, S., Wirzenius, M., Waltari, M., Hellstrom, M., Schomber, T., Peltonen, R. et al. (2008). Blocking VEGFR-3 suppresses angiogenic sprouting and vascular network formation. *Nature* **454**, 656-660.
- Vodyanik, M. A., Yu, J., Zhang, X., Tian, S., Stewart, R., Thomson, J. A. and Slukvin, I. I. (2010). A mesoderm-derived precursor for mesenchymal stem and endothelial cells. *Cell Stem Cell* **7**, 718-729.
- Zeisberger, S. M., Odermatt, B., Marty, C., Zehnder-Fjallman, A. H., Ballmer-Hofer, K. and Schwendener, R. A. (2006). Clodronate-liposome-mediated depletion of tumour-associated macrophages: a new and highly effective antiangiogenic therapy approach. *Br. J. Cancer* **95**, 272-281.
- Zuk, P. A., Zhu, M., Ashjian, P., De Ugarte, D. A., Huang, J. I., Mizuno, H., Alfonso, Z. C., Fraser, J. K., Benhaim, P. and Hedrick, M. H. (2002). Human adipose tissue is a source of multipotent stem cells. *Mol. Biol. Cell* **13**, 4279-4295.

CD45-Ter119-**CD45-Ter119-CD31+ CD34+**

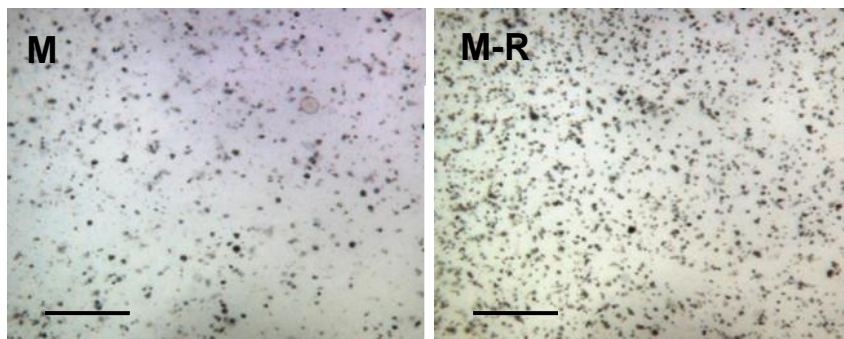
A



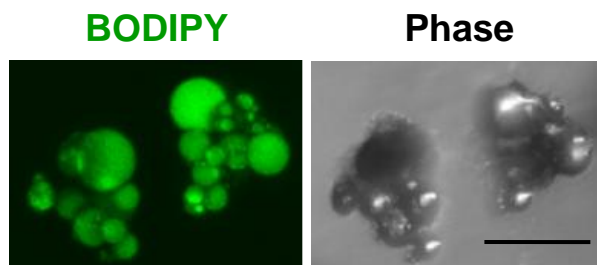
B



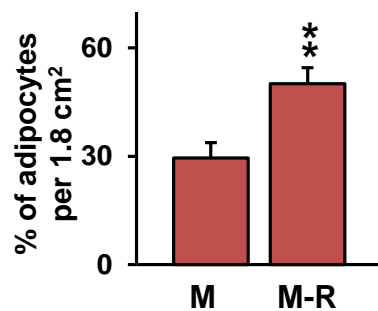
A

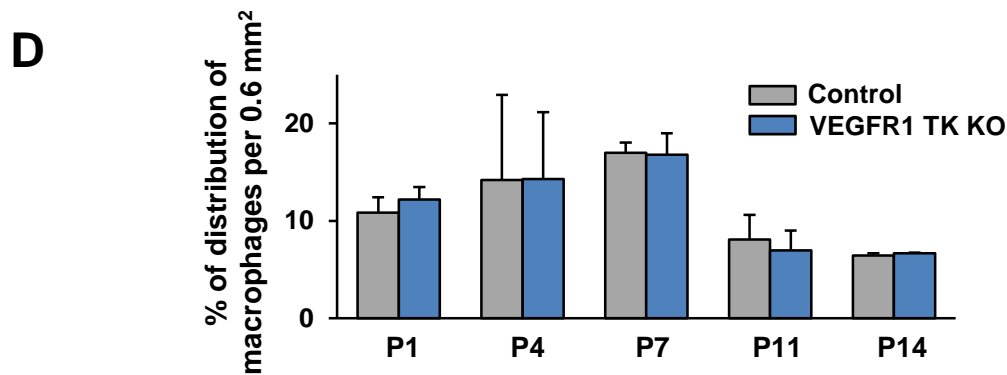
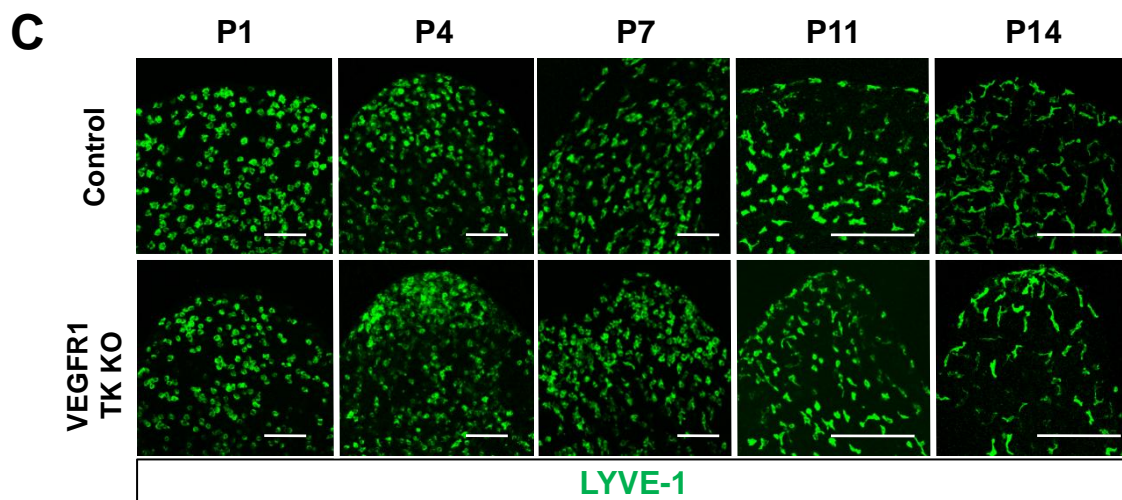
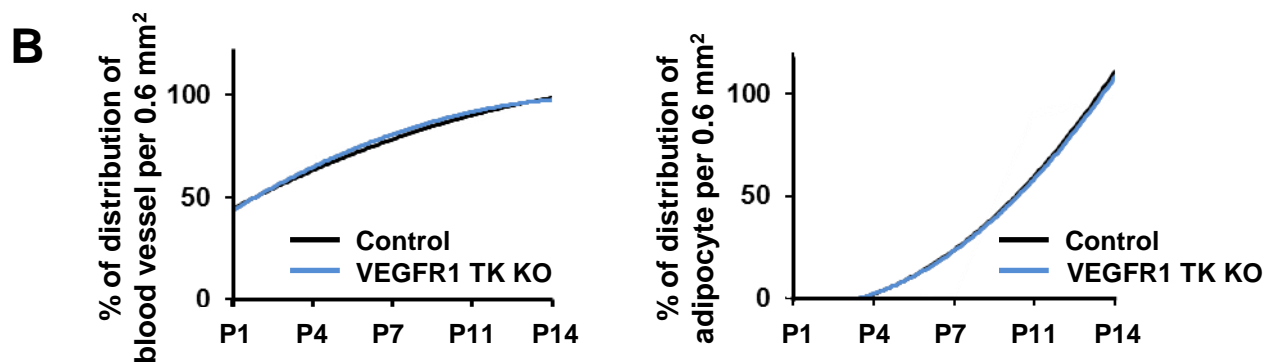
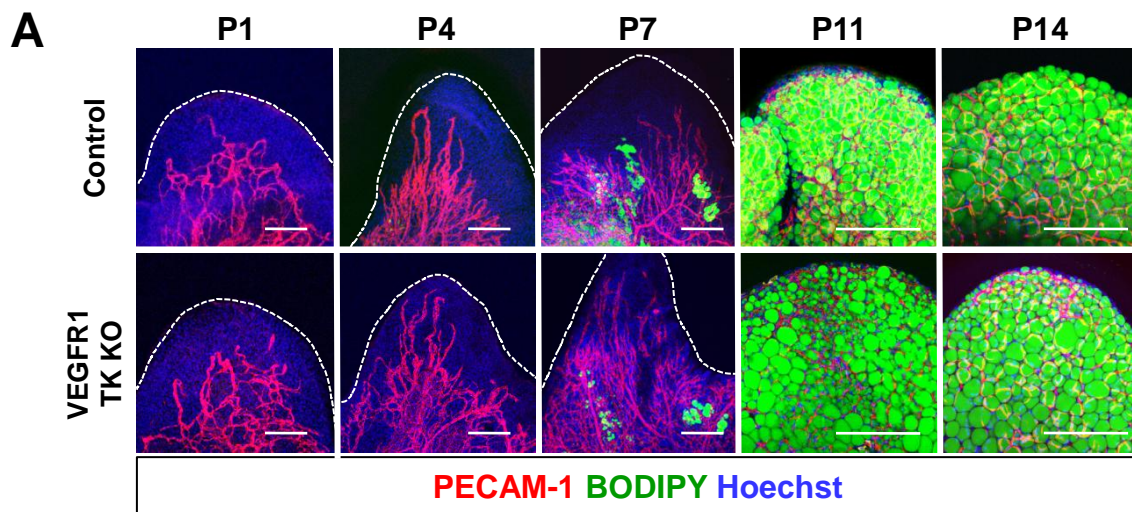


B



C





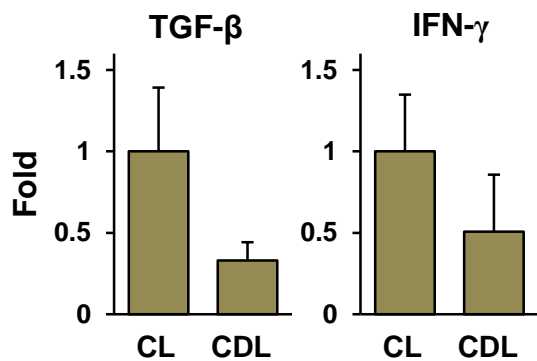
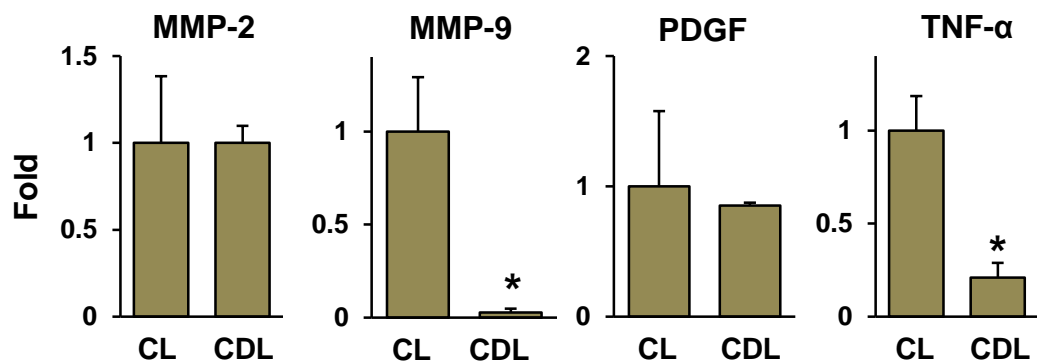
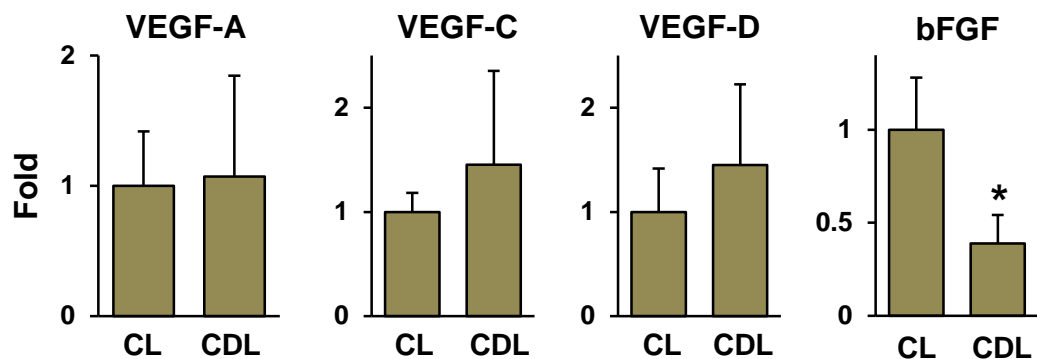


Table S1. Primers (5' to 3') for semi-quantitative and quantitative RT-PCR

Adipogenic genes		
<i>Pparg</i>	Forward	TCCTGTAAAAGCCCGGAGTAT
	Reverse	GCTCTGGTAGGGGCAGTGA
perilipin	Forward	AGATCCCGGCTCTTCAATACC
	Reverse	AGAACCTTGTCAAGGTGCTT
<i>aP2</i>	Forward	GGGGCCAGGCTTCTATTCC
	Reverse	GGAGCTGGGTAGGTATGGG
Osteogenic genes		
<i>Bglap</i>	Forward	GGGCAATAAGGTAGTGAACAG
	Reverse	GCAGCACAGGTCTAAATAGT
<i>Msx2</i>	Forward	TTCACCACATCCCAGCTTCTA
	Reverse	TTGCAGTCTTTTCGCCTTAGC
<i>Runx2</i>	Forward	ATGCTTCATTGCGCTCACAAA
	Reverse	GCACTCACTGACTCGGTTGG
Chondrogenic genes		
<i>Col2a1</i>	Forward	CAGGATGCCCGAAAATTAGGG
	Reverse	ACCACGATCACCTCTGGGT
<i>Col10a1</i>	Forward	CAGCAGCATTACGACCCAAG
	Reverse	CCTGAGAAGGACGAGTGGAC
<i>Acan</i>	Forward	CACGCTACACCCTGGACTTTG
	Reverse	CCATCTCTCTCAGCGAAGCAGT
Adipocyte progenitor genes		
<i>Pref1</i>	Forward	AGTGCGAAACCTGGGTGTC
	Reverse	GCCTCCTTGTTGAAAGTGGTCA
<i>AD-3</i>	Forward	AGCCTAGCCAGATCACAAAGA
	Reverse	CGTCCAGAGGGAACAGTCT
<i>Cebpd</i>	Forward	CGACTTCAGCGCCTACATTGA
	Reverse	CTAGCGACAGACCCACAC
<i>Cd36</i>	Forward	AGAAGGCGGTAGACCAGAC
	Reverse	GTAGGGGGATTCTCCTTGA
Angiogenic factors		
<i>Vegfa</i>	Forward	ACCATGAACTTTCTGCTCTTG
	Reverse	GAAGTTGATCACTTCATGGGACT
<i>Vegfc</i>	Forward	CAGCTAACAAGACATGTCCAACA
	Reverse	CATTGGTTGAGTCATCTTCAACA
<i>Vegfd</i>	Forward	GTCTGTAAAGCACCATGTCCGGGAG
	Reverse	CCACAGGCTGGCTTTCTACTTGCAC
<i>Mmp2</i>	Forward	CAAGTTCCCCGGCGATGTC
	Reverse	TTCTGGTCAAGGTCACCTGTC
<i>Mmp9</i>	Forward	CTGGACAGCCAGACACTAAAG
	Reverse	CTCGCGGCAAGTCTTCAGAG
<i>Ifng</i>	Forward	ATGAACGCTACACACTGCATC
	Reverse	CCATCCTTTGCCAGTTCCTC
<i>Tnfa</i>	Forward	CCCTCACACTCAGATCATCTTCT
	Reverse	GCTACGACGTGGGCTACAG
<i>Tgfb</i>	Forward	CAAGGAGACGGAATACAGGGCTTTC
	Reverse	GTTTCATGTCATGGATGGTGCCAG
<i>bFGF</i>	Forward	CTTGCTATGAAGGAAGATGGACGGC
	Reverse	CCAGTTCGTTTCAGTGCCACATACC
<i>Pdgf</i>	Forward	CACAGAGACTCCGTAGATGAAGATGGG
	Reverse	CACTCGGCGATTACAGCAGGCTCTG
<i>Gapdh</i>	Forward	GGACGCATTGGTCGTCTGG
	Reverse	TTTGCACTGGTACGTGTTGAT